Enhancement of mass transfer conditions to increase the productivity and efficiency of dark fermentation in continuous reactors

Rodolfo Palomo-Briones, L. B. Celis, H. O. Méndez-Acosta, Nicolas Bernet, Eric Trably, E. Razo-Flores

Enhancement of mass transfer conditions to increase the productivity and efficiency of dark fermentation

Rodolfo Palomo-Briones[a], Lourdes B. Celis[a], Hugo O. Méndez-Acosta[b], Nicolas Bernet[c], Eric Trably[c], Elías Razo-Flores[a]*

[a]División de Ciencias Ambientales, Instituto Potosino de Investigación Científica y Tecnológica, San Luis Potosí, S.L.P., México. C.P. 78216. E-mails (in order of appearance): rodolfo.palomo@ipicyt.edu.mx; celis@ipicyt.edu.mx; erazo@ipicyt.edu.mx

[b]Departamento de Ingeniería Química, Centro Universitario de Ciencias Exactas e Ingeniería, Universidad de Guadalajara, Jal., México. C.P. 44430. E-mail: hugo.mendez@cucei.udg.mx

[c]LBE, Univ Montpellier, INRA, Narbonne F-11100, France. E-mail (in order of appearance): nicolas.bernet@inra.fr; eric.trably@inra.fr

*Corresponding author. Telephone: + (52) 444 8342026. E-mail: erazo@ipicyt.edu.mx

ORCID IDs:
Rodolfo Palomo-Briones: 0000-0002-7164-0756
Nicolas Bernet: 0000-0003-2710-3547
Elías Razo-Flores: 0000-0002-8262-695X

Declaration of interest: none

Abstract

Hydrogen (H_2) produced by dark fermentation is an alternative to fulfill the requirements of the transportation sector and to be a complementary source in the forthcoming electricity grid. However, the dark fermentative H_2 production is limited by the accumulation of H_2 in the fermentation broth. In continuous stirred-tank reactors (CSTR), such phenomenon is associated with poor mass transfer conditions. Nevertheless, this parameter has been scarcely considered to enhance H_2 production. In this research, the effect of the H_2 mass transfer conditions on the productivity and efficiency of H_2 production was evaluated using a series of CSTR operated at H_2 mass transfer coefficients (k_La) ranging from 1.04 to 4.23 1/h. The results showed that volumetric H_2 production rate (VHPR) and H_2 yield increased 74 and 78%, respectively, due to enhanced mass transfer conditions. This behavior was driven by 53% decrease of the dissolved H_2 concentration. More specifically, a maximum VHPR of 7.66 L/L-d with a H_2 yield of 1.1 mol H_2/mol hexose was obtained at a k_La = 4.23 1/h. Furthermore, 16S-DGGE analysis and sequencing revealed that *Clostridium* and *Lactobacillus* were the dominant bacterial genera in continuous operation. In particular, *Clostridium* increased its occurrence at k_La of 2.72-4.23 1/h as a response to lower dissolved H_2 concentrations. The novelty of this work relies on the demonstration that mass transfer conditions controls H_2 accumulation and enhances the reactor performance for H_2 production.

Key words: biohydrogen; CSTR; dark fermentation; mass transfer

1. Introduction

The diversification of energy sources is a critical keystone in the contemporaneous vision of sustainable development. In this regard, biofuels are expected to play a relevant role to fulfill future requirements of the transportation sector and to be a complementary source in the forthcoming electricity grid. In this context, molecular hydrogen (H_2) has been underlined due to its high energy content (120 kJ/g) and the highly efficient conversion to electricity through the H_2 fuel-cell technology. Moreover, H_2 can be produced from a wide range of residual biomass through dark fermentation, which also makes it an attractive option in waste valorization scenarios.

The production of H_2 through dark fermentation is achieved by anaerobic microorganisms that use two principal metabolic routes: the pyruvate formate lyase and the pyruvate ferredoxin oxydoreductase pathways [1,2]. These routes are associated with maximum theoretical metabolic yields of 2 and 4 mol H_2/mol hexose, respectively. However, most studies in literature report H_2 yields below these thresholds. The low H_2 production depends on multiple factors, including the microbial community composition, the operational conditions and the efficiency of liquid-gas mass transfer. The importance of this later topic relies on the fact that dissolved H_2 concentration can exert a thermodynamic control on H_2-associated metabolic pathways. For instance, as H_2 accumulates (P_{H2} > 60 Pa), H_2 synthesis from ferredoxin becomes theoretically unfeasible. As a consequence, the maximum H_2 yield decreases from 4 to 2 mol H_2/mol hexose [3]. Further accumulation of H_2 in the liquid phase (P_{H2} > 500 Pa) leads to the occurrence of homoacetogenesis, which is the metabolism through which acetate is synthesized from H_2 and CO_2 [4–6].

In dark fermentative systems, different alternatives have been proposed to enhance H_2 mass transfer [7–13]. Mechanical stirring can be highlighted due to its low-cost and ease of implementation. Using mechanical stirring, Beckers et al. [13] successfully showed that H_2 yield was positively

linked to the increase of the volumetric mass transfer coefficient (k_La), which was controlled in turn by the stirring velocity and gas sparging.

In continuous regime, it can be hypothesized that different steady states of performance could arise as a function of mass transfer conditions with concomitant changes in metabolic pathways and microbial community composition. In this regard, the aim of this work was to compare steady state performances of dark fermentative systems at different conditions of mass transfer (associated with different stirring velocities) with a special focus on the potential shifts in metabolic pathways and microbial communities.

2. Material and methods

2.1 Inoculum and fermentation medium

The seed sludge was obtained from a full-scale UASB reactor treating wastewater from a tequila factory (Casa Herradura, Jalisco, Mexico). Before its use, the sludge was heat treated at 105 °C for 24 h, pulverized in a mortar, and sieved through 0.5 mm mesh. The resulting powder was added to the reactor at a total solids (TS) concentration of 4.5 g TS/L for the startup of CSTR I (Section 2.2).

In all the fermentation experiments, cheese whey powder (CWP) (Darigold, USA) with a lactose content of 75.5% was used as substrate at a fixed inlet concentration of 15 g lactose/L. The fermentation medium was supplemented with the following components as described previously (mg/L) [14]: NH_4Cl, 2110; $MgCl_2 \cdot 6H_2O$, 100; $CuCl_2 \cdot H_2O$, 1.25; $MnCl_2 \cdot 4H_2O$, 7; $FeCl_2 \cdot 4H_2O$, 19.1; $NiCl_2 \cdot 6H_2O$, 102.5. In addition, a phosphate buffer (KH_2PO_4-Na_2HPO_4, pH 5.9) was added to reach a final concentration of 100 mM.

2.2 Bioreactors set-up and operational conditions

A series of five CSTR (Applikon Biotechnologies, USA) with a working volume of 1 L (9.5 cm of internal diameter and 70.88 cm^2 liquid-gas transfer area) was set up as shown in Fig. S1. The bioreactors were equipped with a stirrer and two Rushton-type impellers symmetrically positioned along the depth of the reactor working-volume.

CSTR I was inoculated with the pretreated anaerobic sludge (section 2.1) at a concentration of 4.5 g TS/L and started-up in batch mode for 24 h with an initial substrate concentration of 15 g lactose /L. Stirring, temperature and pH were controlled at 250 rpm, 37 °C and 5.9, respectively. Thereafter, the reactor was switched to continuous mode with a fixed hydraulic retention time (HRT) of 6 h. The reactor was monitored for a minimum of 20 HRT equivalents, i.e. 5 days, and until a steady state was reached in terms of volumetric H_2 production rate (VHPR). The steady state was defined as the phase where the variation of three consecutive measurements was less than 10% of the VHPR. In such state, enough volume of effluent was recovered and centrifuged at 3500 rpm for 10 min at 4°C. The resulting pellets were re-suspended in mineral medium without substrate, characterized in terms of volatile suspended solids (VSS) and stored at -4 °C until their use as inoculum in four more reactors CSTR II to V. CSTR II - V were inoculated with the recovered biomass from CSTR I at a concentration of 0.45 g VSS/L. The start-up strategy and operational conditions were maintained identical to CSTR I, except for the stirring velocity, which was set at 100, 200, 300 and 400 rpm in CSTR II, CSTR III, CSTR IV and CSTR V, respectively. CSTR I – V were also operated and monitored for a minimum of 20 HRT and until stable VHPR was observed.

2.3 Analytical methods

Liquid samples were collected on a regular basis and used to determine the concentrations of biomass, soluble chemical oxygen demand (COD), total carbohydrates and short-chain volatile fatty acids (VFA). Biomass concentration (as volatile suspended solids, VSS) and soluble COD were quantified as described in standard methods [15]. The concentration of total carbohydrates was

110 determined by the phenol sulfuric method [16]. VFA were quantified from filtered (22 µm) samples
111 by capillary electrophoresis (1600A, Agilent Technologies, Waldbronn, Germany) as reported
112 elsewhere [17]. All H_2 and VFAs yields were calculated considering the amount of hexose
113 consumed.

114 Gas production was measured through a liquid displacement device (SEV. Puebla, Mexico), and its
115 composition (H_2 and CO_2) was determined through a gas chromatograph equipped with a thermal
116 conductivity detector (6890N, Agilent Technologies, Waldbronn, Germany). All gas volumes were
117 reported at 1 atm and 273.15 K.

118 2.4 Determination of k_La and dissolved H_2 concentration

119 To determine H_2 mass transfer coefficients (k_La, 1/h) of the CSTR, a series of O_2 desorption
120 experiments were performed at 50, 100, 200, 300 and 400 rpm using the gas-out method described
121 elsewhere [13]. In brief, the reactor vessel was filled with mineral medium without substrate and
122 inoculum. Stirring, temperature and pH were set to 50-400 rpm, 37 °C and 5.9, respectively. The
123 system was assembled with an electrode to measure and record dissolved oxygen (DO)
124 concentrations. For each experiment, the system was first degassed with N_2 and then flushed with
125 pure oxygen until the dissolved O_2 concentration reached 100%. Afterwards, the O_2 sparging was
126 ceased and the decrease of the dissolved gas concentration was recorded until equilibrium was
127 reached. Obtained data were normalized and adjusted to the following desorption equation:

128 $$[DO(t)] = [DO]_{t=0} * e^{-(k_L a)_{O2} * t} \quad (1)$$

129 Where t (h) represents the elapsed time and $(k_L a)_{O_2}$ is the volumetric mass transfer coefficient of
130 O_2. The resulting $(k_L a)_{O_2}$ value altogether with the O_2 and H_2 diffusivities (D_{O_2} and D_{H_2},
131 respectively) were used to compute the $(k_L a)_{H_2}$ considering the following relationship [13]:

$$(k_L a)_{H_2} = (k_L a)_{O_2} * \left({D_{H_2}}/{D_{O_2}} \right)^{1/2} \quad (2)$$

Where D_{H_2} and D_{O_2} were 5.91 x 10^{-5} and 2.62 x 10^{-5} cm^2/s at 40 and 37 °C, respectively [18,19].

Furthermore, to calculate dissolved H_2 concentrations at the different mass transfer conditions, it was first considered that mass transfer of H_2 from the liquid to the gas phase (Q_{H_2}, in mol_{H2}/L-h) can be described as follows:

$$Q_{H_2} = (k_L a)_{H_2} * \left(C_{H_2,liq} - p_{H_2,gas} * H^{cp} \right) \quad (3)$$

Where $(k_L a)_{H_2}$ (1/h) is the volumetric mass transfer coefficient for H_2, $C_{H_2,liq}$ (mol/L) is the concentration of dissolved H_2, $p_{H_2,gas}$ (atm) is the H_2 partial pressure of the headspace, and H^{cp} (mol/L-atm) is the Henry's coefficient of H_2 (8.47 x10^{-4} mol/L-atm at 37°C, Sander, 2015). Solving the equation for $C_{H_2,liq}$ (Eq. 4), we obtain an expression with two known constants (i.e. $k_L a$ and H^{cp}) and two variables that can be derived from bioreactors operation (i.e. Q_{H_2} and $p_{H_2,gas}$).

$$C_{H_2,liq} = {Q_{H_2}}/{\{k_L a\}_{H_2}} + p_{H_2,gas} * H^{cp} \quad (4)$$

2.5 Microbial community analysis

To investigate the microbial community structure and identify potential changes in response to differences of mass transfer conditions, a PCR-DGGE approach was followed as described previously [21]. DNA was extracted from biomass recovered after 24h of batch cultivation (start-up phase) and at the end of each stage using a DNA extraction kit (Zymo-Research, USA). The 16S rRNA gene was amplified by PCR using the 27F (5'-AGAGTTTGATCCTGGCCAG) and 1492R (5'-GGTTACCTTGTTACGACTT) universal primers for bacteria. A nested PCR was conducted with amplicons from the previous stage and primers 357F-GC (5'-

CGCCCGCCGCGCGCGGCGGGCGGGGCGGGGGCACGGGGGGCCTACGGGAGGC AGCAG-3´) and 907R (5'-CCGTCAATTCMTTTGAGTTT) to amplify the V3 - V5 regions. The PCR products were loaded in polyacrylamide gels (8%) with a denaturing gradient (urea-formamide) that ranged from 30 to 60 %. The DGGE electrophoresis conditions were 70 V for 20 h at 60 °C. After electrophoresis, the gel was fixed with acetic acid (10%), treated with a $AgNO_3$ solution (1 g/L) and revealed with a Na_2CO_3 (23.3 g/L) solution. The gel bands were photographed under visible light with a digital camera. The DGGE images were analyzed with the BioNumeric bioinformatics software (Applied Maths, Belgium) to create a presence-absence matrix from which Euclidean distances were calculated. The distances between the DGGE profiles were visualized through a UPGMA dendrogram computed in the R environment [22]. Furthermore, selected DNA bands were cut, reamplified by PCR using 341F (without GC-clamp) and 907R primers, and sequenced by the dideoxynucleotides method in a 3130 Genetic Analyzer (Applied Biosystems, USA). DNA sequences were edited to remove low quality nucleotides with the BioEdit software (Ibis Therapeutics, USA). Edited sequences were compared with the reference 16S-rRNA database of NCBI to find the closest relatives.

2.6 Hydrogen consumption

To evaluate the homoacetogenic activity under the different mass transfer conditions tested, the following mass balance on H_2, acetate and butyrate was performed as suggested elsewhere [23,24]:

$$Homoacetogenic\ acetate = {(2 \cdot Acetate + 2 \cdot Butyrate - Propionate - H_2)}/{6} \quad (5)$$

Where VFA and H_2 are given in mol/d.

To confirm and characterize the H_2 consumption capacity of the microbial community, a series of H_2 consumption experiments was also carried out. These experiments were conducted in 120 mL serum bottles with a working volume of 80 mL, using biomass harvested from the CSTR III (200

rpm) as inoculum. For this purpose, enough volume of effluent was recovered from CSTR III and centrifuged at 3500 rpm for 10 min at 4°C. Resulting pellets were re-suspended in mineral medium (section 2.1), characterized in terms of VSS, and stored at -4 °C until their use. The experiments were prepared with an initial concentration of 2 g VSS/L using the mineral medium with the composition described in section 2.1 and supplemented with 560 mg/L of $NaHCO_3$. No organic substrate was added. The serum bottles were hermetically sealed and the headspace displaced first with N_2 and then with pure H_2. A second set of experiments was prepared identically, but H_2 was pressurized at 1.4 atm. Two additional bottles were prepared, one without biomass and the other without H_2, to serve as physicochemical and endogenous controls, respectively. All experiments were incubated at 37 °C. The H_2 consumption was computed from the decrease of the system pressure and headspace composition.

The cumulative H_2 consumption was modelled utilizing the Gompertz model [25,26]:

$$H_{2_{cummulative}}(t) = H_{max} \cdot exp\left\{-exp\left[\frac{2.71828 \cdot R_{max}}{H_{max}}(\lambda - t) + 1\right]\right\} \quad (6)$$

Where $H_{2_{cumulative}}(t)$ (mmol) is the cumulative H_2 consumed at time t, H_{max} (mmol) is the maximum amount of H_2 consumed in the experiment, R_{max} (mmol/h) is the maximum rate of H_2 consumption, and λ (h) is the lag time before H_2 consumption.

2.7 Statistic analysis

To evaluate the effects of mass transfer conditions on the different response variables of this study, an analysis of variance was conducted. The effect was considered to be significant at a p value lower than 0.05. The response variable was verified to be normally distributed through graphical inspection (q-q plot). The heteroscedasticity was also verified with residual plots. Variables not normally distributed were transformed previously to the analysis. Alternatively, the non-parametric test of Kruskal-Wallis was used. All statistical analysis were conducted with R software [22].

3. Results and discussion

3.1 k_La determination in the dark fermentative system

The $(k_La)_{H_2}$ coefficients, named here "k_La" for simplicity, were determined in accordance with previously reported methodology [13]. The k_La values were in the range of 0.58 - 4.23 1/h and function of the stirring velocity (Supplementary Information Table S1). Such values are specific for the configuration, geometry and specific transfer area of the reactor. Nevertheless, these results are consistent to similar systems as reported elsewhere [13,27]. The subsequent biological experiments were conducted under rpm ≥ 100 rpm to avoid possible stagnation at lower speeds.

3.2 The H_2 mass transfer conditions as a mechanism controlling the productivity and the efficiency of dark fermentation

CSTR I was operated for an equivalent time of 34 HRT (8.5 days) at an organic loading rate (OLR) of 60 g lactose/L-d with the main objective of producing seed-biomass for subsequent experiments (CSTR II - V). The performance of CSTR I was stable in terms of productivity and efficiency, with an average VHPR of 7.1 ± 1.0 L/L-d and H_2 yield of 0.94 ± 0.1 mol H_2/mol hexose. Under similar OLR (55.4 g lactose/L-d), Davila-Vazquez et al. [28] reported a VHPR of 8.8 L/L-d and an H_2 yield of 1.2 mol H_2/mol hexose, which was similar to the results showed in the present work. The stability of H_2 production and the similarity with previous reports were clear indications of a successful establishment of the dark fermentative H_2 production. Thus, the biomass was then recovered to serve as inoculum in the following experiments.

CSTR II to V were independently operated at k_La values in the range of 1.04 to 4.23 1/h, associated with stirring velocities ranging from 100 to 400 rpm (Table S1). The results showed that the mass transfer coefficient strongly affected dark fermentation in terms of VHPR ($F_{3,\,50}$=13.05, $p<0.05$) and H_2 yield ($F_{3,\,50}$=13.04, $p<0.05$) (Fig. 1). At the lowest k_La tested (1.04 1/h), the VHPR was 4.4 ± 1.3

221 L/L-d with an H_2 yield of 0.6 ± 0.15 mol H_2/mol hexose. In contrast, at the highest value of k_La
222 (4.23 1/h), an average VHPR of 7.66 ± 1.42 L/L-d was obtained with an H_2 yield of 1.08 ± 0.21 mol
223 H_2/mol hexose. These results represent an increase of 74% in terms of VHPR and 78% in terms of
224 H_2 yield.

225 The extent of improvement, in both VHPR and H_2 yield, achieved in this work was consistent with
226 previous reports that focused on H_2 mass transfer (Table S2). For instance, Beckers et al. [13]
227 reported an improvement of approximately 89 and 19 % in terms of H_2 production rate and H_2
228 yield, respectively, in an anaerobic stirred tank reactor after having increased the stirring conditions
229 from 0 to 400 rpm. Using CO_2 sparging, Kim et al. [7] were able to increase the VHPR and H_2 yield
230 in a CSTR by 56% and 118%, respectively. Nevertheless, such an approach resulted in H_2 dilution,
231 which is not convenient for practical applications. In comparison, with optimized mixed conditions
232 reported in the present work, remarkable increases in the VHPR and H_2 yield were reached,
233 avoiding the utilization of additional gases and, therefore, the H_2 produced remains concentrated.

234 3.3 Enhancement of mass transfer conditions intensifies metabolic routes leading to H_2 production

235 To investigate the influence of mass transfer conditions on metabolic pathways, main VFA (i.e.
236 formate, acetate, butyrate and lactate) concentrations were determined at the different conditions of
237 stirring velocities. Results revealed that the enhancement of H_2 mass transfer performance was
238 accompanied by an increase of the VFA molar yield. In particular, significant differences in acetate
239 and butyrate production yields (Fig. 1 A and B) were observed due to the enhancement of H_2
240 transfer conditions. In CSTR II, with k_La of 1.04 1/h, the production of acetate and butyrate was
241 0.29 and 0.31 mol/mol hexose, respectively. Meanwhile, in CSTR V, with k_La of 4.23 1/h, the
242 acetate and butyrate yields increased up to 0.44 and 0.5 mol/mol hexose, respectively. This finding
243 is consistent with the fact that the acetate and butyrate pathways are the most efficient routes in
244 terms of H_2 production by dark fermentation.

On the other hand, H_2 concentrations in the fermentation broth (Fig. 2 C) clearly indicated that the increase of acetate and butyrate yields were associated with the change of mass transfer conditions and the subsequent decrease of dissolved H_2. The theoretical H_2 concentrations in the fermentation liquid were in the range of 7.5 to 3.4 mmol H_2/L, with the lowest value at the k_La of 4.23 1/h. Nevertheless, considering the results of VFA and dissolved H_2 concentration, as well as the VHPR and H_2 yield (Fig. 1), it seemed that mass-transfer did not affect H_2 metabolism beyond a k_La of 2.6 1/h, i.e. 300 rpm. Thus, the operation at 300 rpm was considered as the most suitable stirring velocity for this type of reactor.

3.4 Microbial community

The analysis of the 16S rRNA-DGGE (Fig. 3) and the sequencing results (Table 1) showed that the microbial community was mainly composed of *Clostridium* and *Lactobacillus* species. These two genera have been previously reported to play important roles in dark fermentative systems [14,29,30]. *Clostridium spp.* are mostly related to H_2-producing bacteria and are widely found in dark fermentative systems associated with high efficiencies (e.g. [1,31]). In contrast, *Lactobacillus spp.* correspond to lactic acid bacteria that have been identified as substrate competitors of H_2-producers during the fermentation of cheese whey [32]. Moreover, it has been shown that the abundance of lactic acid bacteria increased under relatively high organic loading rates (58.8 and 88.2 g lactose/L-d), and it was likely associated with the accumulation of H_2 in the fermentative medium [29].

Interestingly, the DGGE analysis showed that *Lactobacillus* (band at DGGE relative distance ~ 68) was more abundant in the samples taken at the end of CSTRs operation (Fig. 3), suggesting that these microorganisms were enriched during the H_2 production process. DGGE profiles also revealed that bands associated with *Clostridium* (two bands at DGGE relative distances of 45 and 50, approximately) were less intense in the samples taken at the end of CSTR II and CSTR III (1.04

and 1.64 1/h) than those taken in CSTR IV and CSTR V (2.72 and 4.23 1/h). Altogether, these findings indicate that H_2 transfer conditions did not only affect the productivity, efficiency and metabolism in dark fermentative systems, but they have also important implications on shaping microbial communities of dark fermentation.

3.5 The dual capacity of hydrogenogenic microorganisms

As largely reported, several dark fermentative species issued from the *Clostridium* genus have the capacity to consume H_2 through the homoacetogenesis pathway in response to high dissolved H_2 concentrations. To quantify this activity in mixed cultures, previous studies reported an approach based on balancing the acetate, butyrate and H_2 productivities [23,24]. In accordance with this method, it was found that homoacetogenic acetate production rates ranged from 31.1 to 68.6 mol acetate/L-d. In terms of percentage, the acetate produced by homoacetogenesis was 32-46 % of total acetate quantified in the systems (Table 2). Similar values were reported elsewhere by Luo et al. [24] at different conditions of pH, temperature and sludge pretreatment. Also, in UASB reactors, Carrillo-Reyes et al. [33] reported homoacetogenic productivities that represented about 50% of the total acetate observed. In regard to homoacetogenesis estimation, it is important to mention that its theoretical evaluation is subjected to uncertainties that are difficult to control: 1) homoacetogenesis is carried out through the Wood-Ljundahl pathway, which could theoretically lead to other not considered metabolites, e.g. ethanol and propionate [34], and 2) the mass balance assumes that acetate is associated with a H_2 molar yield of 4 mol H_2/mol hexose, which is not accurate in most of the cases.

To confirm the dual characteristics of dark fermentative microorganisms and propose a method to avoid uncertainties of homoacetogenesis estimation, biomass harvested from a H_2-producing reactor (CSTR III) was used to perform additional experiments to study the consumption of H_2. The results showed that the H_2 consumption profile was successfully modeled with the Gompertz equation

(Fig. 4). The corresponding kinetic parameters are presented in Table 3. Interestingly, the system with an initial pressure of 1.4 atm showed remarkably higher velocity of H_2 uptake in comparison with the system at 1 atm. This finding confirms that H_2 accumulation controls the metabolism leading to its own consumption. Furthermore, the capillary electrophoresis analysis revealed that acetate was the main metabolite, produced at final concentrations of 94.8 ± 39 and 175 ± 46 mg/L in the system with an initial pressure of 1 and 1.4 atm, respectively.

4. Conclusions

This research demonstrates that the dark fermentation pathways and the related microbial communities can be controlled by improving H_2 mass transfer conditions. It was found that the increase of the mass transfer coefficient, k_La, enhanced the VHPR from 4.4 ± 1.3 L/L-d at a k_La of 1.04 1/h (100 rpm) to 7.6 ± 1.4 L/L-d at k_La of 4.23 1/h (400 rpm), which is equivalent to a 74 % increase. Similarly, the H_2 yield shifted from 0.6 ± 0.15 mol H_2/mol hexose to 1.08 ± 0.21 mol H_2/mol hexose, i.e. an increment of 78%. The improvement in mass transfer conditions produced lower concentrations of dissolved H_2, which favored the dominance of *Clostridium sp.* over *Lactobacillus sp.*, which led to an enhancement of H_2 production through the acetate and butyrate pathways. The dual capability of the hydrogenogenic biomass was confirmed through microcosm studies that allowed to develop a first approach towards the characterization of H_2 consuming mixed cultures. Overall, it was demonstrated that the dark fermentation could be successfully controlled by mass transfer conditions.

Acknowledgements

This work was financially supported by Fondo Sectorial SENER-CONACYT Sustentabilidad Energética, Clúster Biocombustibles Gaseosos (project 247006). The authors acknowledge Esmeralda Nguyen López-Lozano for the kind revision of the manuscript and the technical assistance of Dulce Partida Gutiérrez, Guillermo Vidriales Escobar, Juan Pablo Rodas Ortíz and

Viviana Ruiz-Diaz. Rodolfo Palomo Briones is also thankful for the PhD scholarship provided by CONACYT.

Appendix A. Supplementary material.

References

[1] Cabrol L, Marone A, Tapia-Venegas E, Steyer J-P, Ruiz-Filippi G, Trably E. Microbial ecology of fermentative hydrogen producing bioprocesses: useful insights for driving the ecosystem function. FEMS Microbiol Rev 2017;41:158–81. doi:10.1093/femsre/fuw043.

[2] Bharathiraja B, Sudharsanaa T, Bharghavi A, Jayamuthunagai J, Praveenkumar R. Biohydrogen and Biogas – An overview on feedstocks and enhancement process. Fuel 2016;185:810–28. doi:10.1016/j.fuel.2016.08.030.

[3] Angenent LT, Karim K, Al-Dahhan MH, Wrenn B a., Domíguez-Espinosa R. Production of bioenergy and biochemicals from industrial and agricultural wastewater. Trends Biotechnol 2004;22:477–85. doi:10.1016/j.tibtech.2004.07.001.

[4] Saady NMC. Homoacetogenesis during hydrogen production by mixed cultures dark fermentation: Unresolved challenge. Int J Hydrogen Energy 2013;38:13172–91. doi:10.1016/j.ijhydene.2013.07.122.

[5] Demirel B, Scherer P. The roles of acetotrophic and hydrogenotrophic methanogens during anaerobic conversion of biomass to methane: a review. Rev Environ Sci Bio/Technology 2008;7:173–90. doi:10.1007/s11157-008-9131-1.

[6] Liu R, Hao X, Wei J. Function of homoacetogenesis on the heterotrophic methane production with exogenous H2/CO2 involved. Chem Eng J 2016;284:1196–203. doi:10.1016/j.cej.2015.09.081.

[7] Kim DH, Han SK, Kim SH, Shin HS. Effect of gas sparging on continuous fermentative hydrogen production. Int J Hydrogen Energy 2006;31:2158–69. doi:10.1016/j.ijhydene.2006.02.012.

[8] Chang S, Li J, Liu F, Yu Z. Effect of different gas releasing methods on anaerobic fermentative hydrogen production in batch cultures. Front Environ Sci Eng 2012;6:901–6. doi:10.1007/s11783-012-0403-1.

[9] Bakonyi P, Buitrón G, Valdez-Vazquez I, Nemestóthy N, Bélafi-Bakó K. A novel gas separation integrated membrane bioreactor to evaluate the impact of self-generated biogas recycling on continuous hydrogen fermentation. Appl Energy 2017;190:813–23. doi:10.1016/j.apenergy.2016.12.151.

[10] Lee K-S, Tseng T-S, Liu Y-W, Hsiao Y-D. Enhancing the performance of dark fermentative hydrogen production using a reduced pressure fermentation strategy. Int J Hydrogen Energy 2012;37:15556–62. doi:10.1016/j.ijhydene.2012.04.039.

[11] Kisielewska M, Dębowski M, Zieliński M. Improvement of biohydrogen production using a reduced pressure fermentation. Bioprocess Biosyst Eng 2015;38:1925–33. doi:10.1007/s00449-015-1434-3.

[12] Contreras-Dávila CA, Méndez-Acosta HO, Arellano-García L, Alatriste-Mondragón F, Razo-Flores E. Continuous hydrogen production from enzymatic hydrolysate of Agave tequilana bagasse: Effect of the organic loading rate and reactor configuration. Chem Eng J 2017;313:671–9. doi:10.1016/j.cej.2016.12.084.

[13] Beckers L, Masset J, Hamilton C, Delvigne F, Toye D, Crine M, et al. Investigation of the links between mass transfer conditions, dissolved hydrogen concentration and biohydrogen production by the pure strain Clostridium butyricum CWBI1009. Biochem Eng J 2015;98:18–28. doi:10.1016/j.bej.2015.01.008.

[14] Palomo-Briones R, Razo-Flores E, Bernet N, Trably E. Dark-fermentative biohydrogen pathways and microbial networks in continuous stirred tank reactors: Novel insights on their control. Appl Energy 2017;198:77–87. doi:10.1016/j.apenergy.2017.04.051.

[15] APHA/AWWA/WEF. Standard Methods for the Examination of Water and Wastewater. 2012.

[16] Dubois M, K.A.Gilles, J.K.Hamilton, P.A.Rebers, Fred.Smith. Colorimetric Method for Determination of Sugars and Related Substances. Anal Chem 1956;28:350–6. doi:10.1021/ac60111a017.

[17] Davila-Vazquez G, Alatriste-Mondragón F, de León-Rodríguez A, Razo-Flores E. Fermentative hydrogen production in batch experiments using lactose, cheese whey and glucose: Influence of initial substrate concentration and pH. Int J Hydrogen Energy 2008;33:4989–97. doi:10.1016/j.ijhydene.2008.06.065.

[18] Ferrell RT, Himmelblau DM. Diffusion coefficients of hydrogen and helium in water. AIChE J 1967;13:702–8. doi:10.1002/aic.690130421.

[19] Han P, Bartels DM. Temperature Dependence of Oxygen Diffusion in H 2 O and D 2 O †. J Phys Chem 1996;100:5597–602. doi:10.1021/jp952903y.

[20] Sander R. Compilation of Henry's law constants (version 4.0) for water as solvent. Atmos Chem Phys 2015;15:4399–981. doi:10.5194/acp-15-4399-2015.

[21] Carrillo-Reyes J, Celis LB, Alatriste-Mondragón F, Razo-Flores E. Different start-up strategies to enhance biohydrogen production from cheese whey in UASB reactors. Int J Hydrogen Energy 2012;37:5591–601. doi:10.1016/j.ijhydene.2012.01.004.

[22] R Development Core Team R. R: A Language and Environment for Statistical Computing. vol. 1. 2011. doi:10.1007/978-3-540-74686-7.

[23] Arooj M, Han S, Kim S, Kim D, Shin H. Continuous biohydrogen production in a CSTR using starch as a substrate. Int J Hydrogen Energy 2008;33:3289–94. doi:10.1016/j.ijhydene.2008.04.022.

[24] Luo G, Karakashev D, Xie L, Zhou Q, Angelidaki I. Long-term effect of inoculum pretreatment on fermentative hydrogen production by repeated batch cultivations: Homoacetogenesis and methanogenesis as competitors to hydrogen production. Biotechnol Bioeng 2011;108:1816–27. doi:10.1002/bit.23122.

[25] Zwietering MH, Jongenburger I, Rombouts FM, van 't Riet K. Modeling of the bacterial growth curve. Appl Environ Microbiol 1990;56:1875–81. doi:0099-2240/90/061875-07$02.00/0.

[26] Ginkel S Van, Sung S, Lay J-J. Biohydrogen Production as a Function of pH and Substrate

Concentration. Environ Sci Technol 2001;35:4726–30. doi:10.1021/es001979r.

[27] de Kok S, Meijer J, van Loosdrecht MCM, Kleerebezem R. Impact of dissolved hydrogen partial pressure on mixed culture fermentations. Appl Microbiol Biotechnol 2013;97:2617–25. doi:10.1007/s00253-012-4400-x.

[28] Davila-Vazquez G, Cota-Navarro CB, Rosales-Colunga LM, de León-Rodríguez A, Razo-Flores E. Continuous biohydrogen production using cheese whey: Improving the hydrogen production rate. Int J Hydrogen Energy 2009;34:4296–304. doi:10.1016/j.ijhydene.2009.02.063.

[29] Palomo-Briones R, Trably E, López-Lozano NE, Celis LB, Méndez-Acosta HO, Bernet N, et al. Hydrogen metabolic patterns driven by Clostridium-Streptococcus community shifts in a continuous stirred tank reactor. Appl Microbiol Biotechnol 2018;102:2465–75. doi:10.1007/s00253-018-8737-7.

[30] García-Depraect O, León-Becerril E. Fermentative biohydrogen production from tequila vinasse via the lactate-acetate pathway: Operational performance, kinetic analysis and microbial ecology. Fuel 2018;234:151–60. doi:10.1016/j.fuel.2018.06.126.

[31] Etchebehere C, Castelló E, Wenzel J, del Pilar Anzola-Rojas M, Borzacconi L, Buitrón G, et al. Microbial communities from 20 different hydrogen-producing reactors studied by 454 pyrosequencing. Appl Microbiol Biotechnol 2016;100:3371–84. doi:10.1007/s00253-016-7325-y.

[32] Ferreira Rosa PR, Carrer Gomes B, Amâncio Varesche MB, Luiz Silva E. Characterization and antimicrobial activity of lactic acid bacteria from fermentative bioreactors during hydrogen production using cassava processing wastewater. Chem Eng J 2016;284:1–9. doi:10.1016/j.cej.2015.08.088.

[33] Carrillo-Reyes J, Celis LB, Alatriste-Mondragón F, Razo-Flores E. Decreasing methane production in hydrogenogenic UASB reactors fed with cheese whey. Biomass and Bioenergy 2014;63:101–8. doi:10.1016/j.biombioe.2014.01.050.

[34] Liu C, Luo G, Wang W, He Y, Zhang R, Liu G. The effects of pH and temperature on the acetate production and microbial community compositions by syngas fermentation. Fuel 2018;224:537–44. doi:10.1016/j.fuel.2018.03.125.

427 Legends to figures

428

429 Fig. 1. Improvement of A) volumetric hydrogen production rate and B) H_2 yield as results of the
430 modification of the hydrogen mass transfer coefficient (k_La) through stirring velocity. Boxes with
431 same letters are not significant different at $p<0.05$ in accordance with the Tukey test.

432

433 Fig. 2. Effect of the hydrogen mass transfer coefficient (k_La) on A) the fermentative byproducts, B)
434 total volatile fatty acids concentration, and C) dissolved hydrogen concentrations.

435

436 Fig. 3. DGGE (Denaturing gradient gel electrophoresis) profiles from dark fermentation systems
437 operated under different mass transfer conditions. Groups with a euclidean distance among its
438 members <1 are colored to aid in the figure interpretation. Band numbers indicate sequenced
439 samples (see Table 1).

440

441 Fig. 4. Hydrogen consumption profiles utilizing hydrogenogenic biomass harvested from the
442 continuous stirred-tank reactor III. Experimental points (□), physicochemical control (-Δ-) and
443 gompertz model (- - -). A) Experiment performed at an initial P_{H2} of 1 atm. B) Experiment
444 performed at an initial P_{H2} of 1.4 atm.

445

Table 1

Table 1. Affiliation of DGGE (denaturing gradient gel electrophoresis) bands from samples taken under different mass transfer conditions.

Band	Closest relative (order/family/genus/species)	Identity	Accession No.
1	*Clostridiales/Clostridiaceae/Clostridium/ C. butyricum*	549/551 (99%)	NR_113244.1
2	*Clostridiales/Clostridiaceae/Clostridium/ C. butyricum*	551/551 (100%)	NR_113244.1
3	*Clostridiales/Clostridiaceae/Clostridium/ C. butyricum*	438/441 (99%)	NR_113244.1
4	*Clostridiales/Ruminococcaceae/Caproiciproducens/ C. galactitolivorans*	470/478 (98%)	NR_145929.1
5	*Clostridiales/Ruminococcaceae/Caproiciproducens/ C. galactitolivorans*	336/352 (95%)	NR_145929.1
6	*Bacillales/Sporolactobacillaceae/ Sporolactobacillus/ S. nakayamae*	339/352 (96%)	NR_114001.1
7	*Clostridiales/Clostridiaceae/Clostridium/ C. jeddahense*	549/553 (99%)	NR_144697.1
8	*Bacillales/Sporolactobacillaceae/Sporolactobacillus/ S. terrae*	457/470 (97%)	NR_112772.1
9	*Clostridiales/Clostridiaceae/Clostridium/ C. butyricum*	555/562 (99%)	NR_113244.1
10	*Clostridiales/Clostridiaceae/Clostridium/ C. butyricum*	542/548 (99%)	NR_113244.1
11	*Clostridiales/Clostridiaceae/Clostridium/ C. butyricum*	551/551 (100%)	NR_113244.1
12	*Lactobacillales/Lactobacillaceae/ Lactobacillus/ L. paracasei*	543/543 (100%)	NR_113337.1
13	*Lactobacillales/Lactobacillaceae/ Lactobacillus/ L. paracasei*	546/547 (99%)	NR_113337.1
14	*Enterobacterales/Enterobacteriaceae/Klebsiella/ K. variicola*	528/529 (99%)	NR_025635.1

Table 2. Theoretical determinations of H_2 consumption by homoacetogenesis.

Stirring	kLa	VHPR	H_2 yield	Homoacetogenesis			
(rpm)	(1/h)	(L/L-d)	(mol H_2/mol hexose)	(mol acetate/L-d)	% of total acetate	(L H_2-eq/L-d)[a]	% of theoretical H_2[b]
100	1.04	4.40	0.61	31.1	32	2.79	39%
200	1.64	5.60	0.73	61.1	46	5.47	49%
300	2.72	7.67	1.00	68.6	38	6.15	44%
400	4.23	7.66	1.08	45.8	33	4.10	35%

VHPR: Volumetric hydrogen production rate

[a]Accounts the amount of H_2 consumed in the synthesis of homoacetogenic acetate

[b]Estimates the percentage of H_2 that is lost by the homoacetogenic route

Table 3. Summary of H_2 consumption experiments. For both experimental conditions, two additional serum bottles were set-up to account for the inoculum activity (without the addition of H_2 gas) and the contribution of physicochemical phenomena (e.g. mass transfer).

Experiment	Initial pressure (atm)	Gompertz parameters			pH final	Acetate concentration (mg/L)
		H_{max} ($mmol_{H2}$)	R_{max} (mmol H_2/h)	λ (h)		
A (n=3)	1	12.64	0.75	9.49	5.47 ± 0.02	94.9 ± 39
B (n=3)	1.4	17.87	1.24	12.52	5.44 ± 0.19	175 ± 46

Figure 1

Click here to download high resolution image

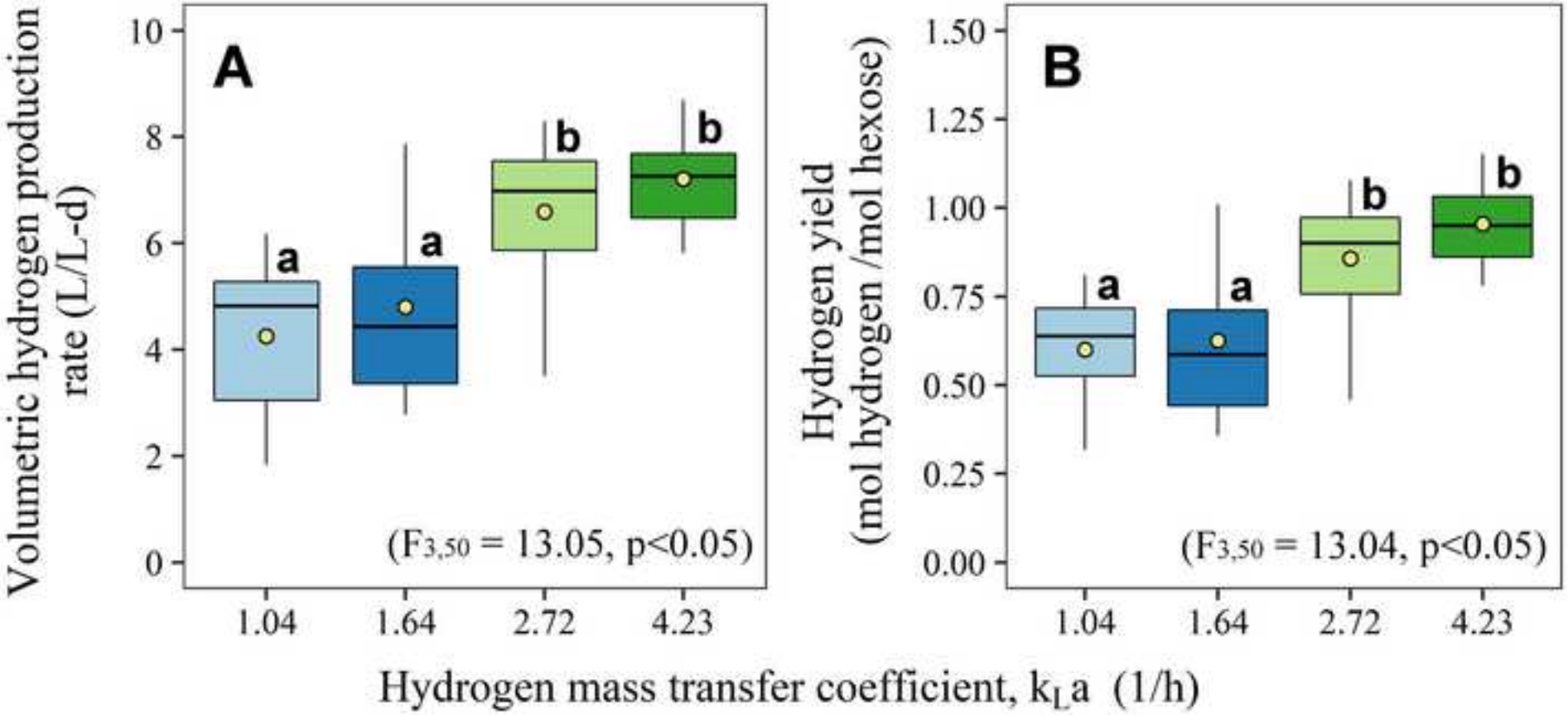

Figure 2

Click here to download high resolution image

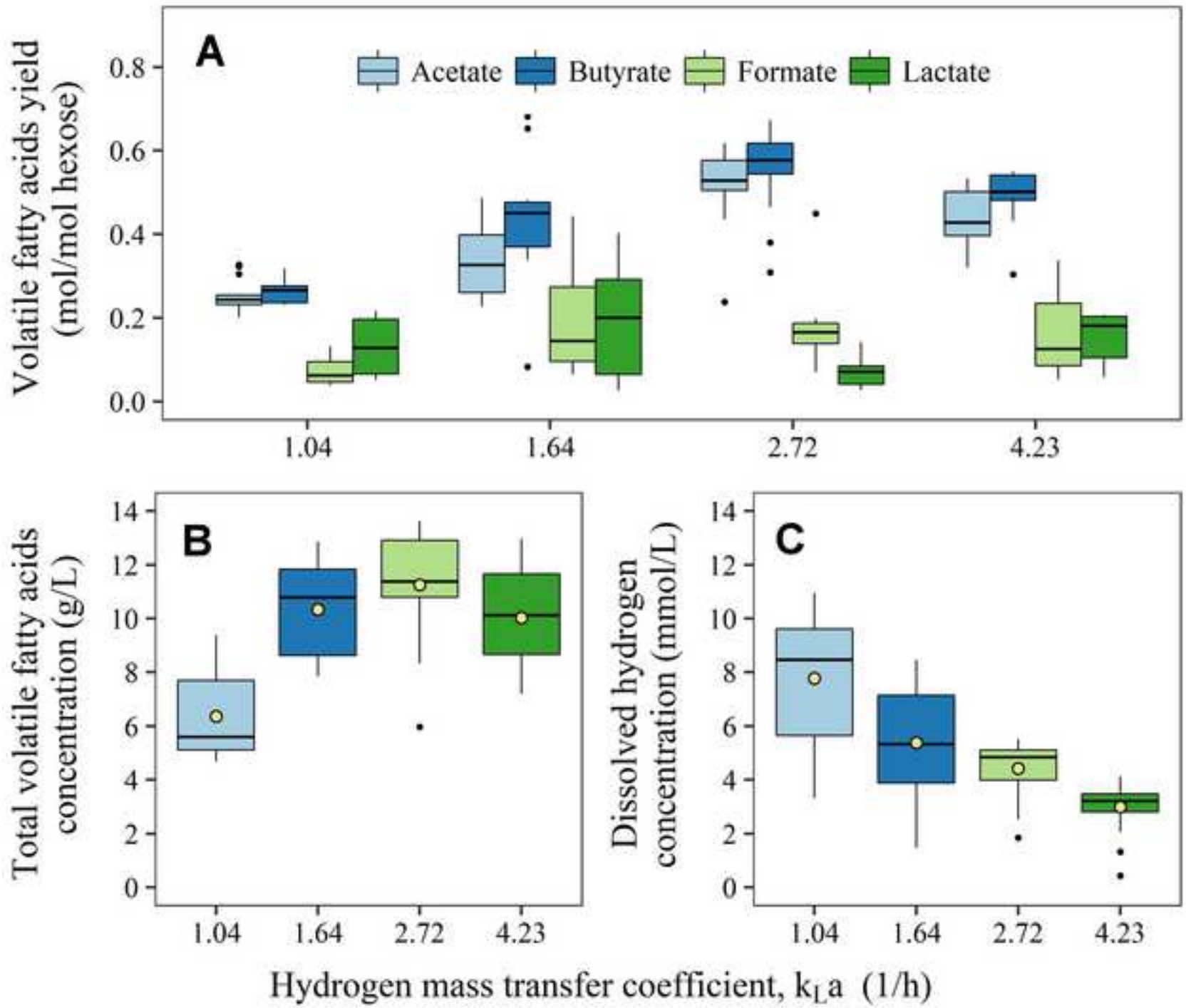

Figure 3

Click here to download high resolution image

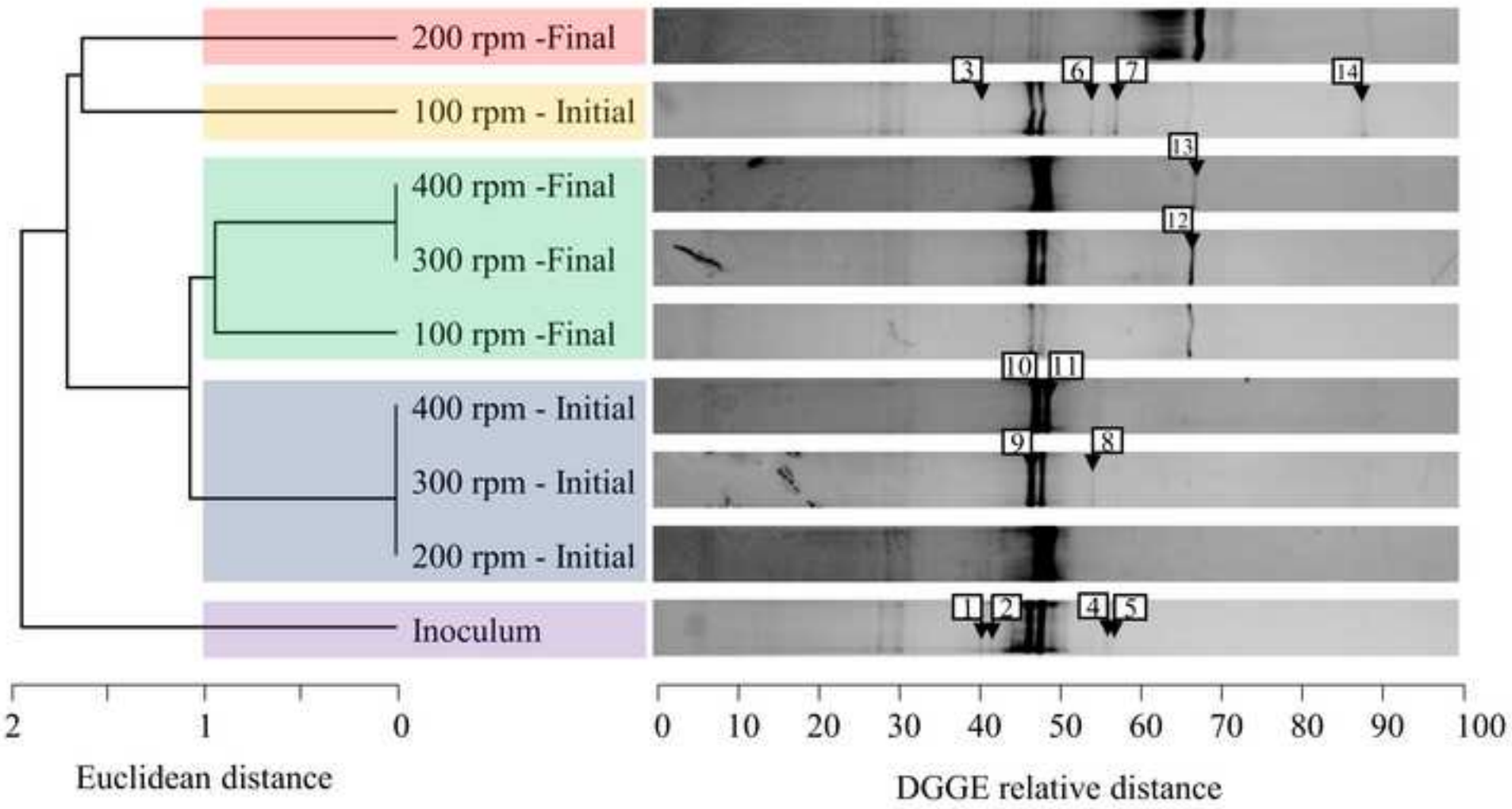

Figure 4

Click here to download high resolution image